Available online at www.academicpaper.org

Academic @ Paper

ISSN 2146-9067

International Journal of Automotive Engineering and Technologies

Vol. 4, Issue 3, pp. 152 – 161, 2015

Original Research Article

International Journal of Automotive Engineering and Technologies

http://www.academicpaper.org/index.php/IJAET

Computational Study of EGR and Excess Air Ratio Effects on a Methane Fueled CAI Engine

Melih Yıldız[1*], S.Orhan Akansu[1], Bilge Albayrak Çeper[1]

[1] Erciyes University Faculty of Eng.,Dept.of Mech.Eng., 38039 Kayseri, Turkey

Received 17 October 2015 Accepted 30 October 2015

Abstract

This paper presents the numerical analysis of a controlled auto ignition (CAI), four stroke, single cylinder engine, by using methane fuel. The goal of this study was to determine how exhaust gas recirculation (EGR) rate affects combustion, emission and engine performance. The EGR rates were selected as 27 %, 32 %, 37 %, and 42 % by mass with excess air ratios of 1.0, 1.5, 2.0, and 2.5. An in-cylinder temperature of 570 K was considered at intake valve closing time (IVC) and an engine speed of 1500 rpm was used for all cases. The Computational Fluid Dynamics (CFD) code FLUENT was used for numerical analysis. The numerical modeling was solved by taking into consideration the effect of turbulence, by using the Renormalization Group Theory (RNG) k-ε model.

The results indicate that increase in EGR rate and excess air ratio have significant effects on in-cylinder pressure, temperature, heat release rate, pressure rise rate, combustion duration, brake work, specific NOx and CO emissions, thermal efficiency and specific fuel consumption. Moreover, CAI combustion resulted in a rapid heat release rate which gives rise to an increase in the pressure rise rate, high temperature value and high level SNOx emission, when EGR rate was low level (up to 32 %) for excess air ratio(λ) value of 1 and 1.5. To achieve CAI combustion resulting in low level SNOx emission, the mixture must include an EGR rate of more than 32 % or become leaner.

Key words: CAI, CFD, EGR, methane, heat release rate

Abbreviations

ATDC	after top dead center
BTDC	before top dead center
CAD	crank angle degree
CAI	controlled auto ignition
CI	compressed ignition
CO2	carbon dioxide
EGR	exhaust gas recirculation
HCCI	homogeneous charged compressed ignition
HRR	heat release rate
PRR	pressure rise rate
SCO	specific carbon monoxide emission
SFC	specific fuel consumption
SI	spark ignition
SNOx	specific nitrogen oxide emission
λ	excess air ratio
θ	crank angle
γ	specific heats ratio
η_{th}	thermal efficiency

*Corresponding Author:
E-mail: melihyildiz@erciyes.edu.tr

Note: This paper has been presented at the International Conference on Advanced Technology & Sciences (ICAT'15) held in Antalya (Turkey).

1. Introduction

Controlled auto-ignition (CAI) or homogeneous charged compressed ignition (HCCI) combustion promising low level NOx emission and improvement in fuel economy is an advanced combustion technology alternative to SI and CI combustion. CAI/HCCI combustion relies heavily on a chemical kinetic process characterized by nearly simultaneous oxidation of lean or diluted mixture in a cylinder [1]. In principle, the fuel and air in a CAI/HCCI engine are mixed together either in the intake port or in the cylinder with direct injection. The premixed charge is compressed and at the end of the compression stroke, combustion is initiated by auto-ignition in a similar way to a conventional CI engine [2]. CAI/HCCI combustion, therefore, includes properties of both the SI and CI combustion engine process. However, CAI/HCCI combustion restricts the range of engine operation conditions due to its characteristics, rapid heat release and challenges of the auto-ignition timing control, while having the potential for lower NOx emission and improved thermal efficiency at certain operating conditions. In order to cope with limited operation range (knocking, misfire, partial burn), various methods such as heating intake air, higher compression ratio, more auto-ignitable fuel and exhaust gas recirculation [3],[4],[5] have been used. Among these methods, the exhaust gas recirculation method provided by exhaust gas rebreathing, in which exhaust gas is trapped by means of using a negative valve overlap strategy [6],[7],[8],[9] seems to be the most practical and effective way without modification of the compression ratio, heating intake air[10].

The EGR in the charge, generally, influences with the heating effect, the dilution effect, the heat capacity effect and the chemical effect on CAI engines [11].Therefore, the change of EGR rate in a CAI engine affects combustion phasing directly bringing about a change in engine performance and emission. Recently, many studies have been performed to determine the effect of EGR rate and to enhance the range of CAI/HCCI engine operation.

Yap et al.[12] investigated HCCI engine operation to present the application of the residual gas trapping strategy to propane HCCI and the usable operation range of the engine. This study showed that the residual gas trapping method is an effective method in reducing intake temperature requirement with HCCI combustion. The compression ratio of 15 with the residual gas trapping HCCI operation can also be achieved without inlet heating due to the heating effect of residual gas and the higher temperature in the cylinder rising with high compression ratio.

Zhoa et al.[13] achieved stable CAI combustion without increasing the compression ratio and intake charge heating. They used variable camshaft timings to adjust the EGR rate in a 1.7 lt, four stroke cylinders, with a compression ratio of 10 and fueled by gasoline. Fathi et al.[14] studied the influence of EGR on the combustion and emission of an HCCI combustion engine fueled with n-heptane/natural gas. They concluded that combustion phasing alters with EGR, since auto-ignition is delayed and the combustion duration is prolonged by applying more EGR.

Ghorbanpour and Rasekhi[15] studied the effect of various operation variables on a diesel HCCI engine numerically by using a CFD model through AVL Fire software. A turbulence model was used employing the RNG k-ε method and the Zeldovich mechanism was used for the NOx formation in their study. By using the Kennedy–Hiroyasu-Magnussen model, soot emission was also investigated.Chen and Milovanovic [16] analyzed numerically both the thermal and chemical effects of the hot EGR on HCCI combustion by using the combustion simulation package SENKIN. They stated that the thermal energy contained in the EGR is essential for combustion initiation, but the chemical species in EGR have different effects on both ignition timing and heat release rate.

In this study, the performance and emission

parameters of a CAI engine with different EGR rate was numerically investigated by using the Computational Fluid Dynamics (CFD) code FLUENT. This study focused on analysis of in-cylinder pressure and temperature, heat release, pressure rise rate, combustion duration, thermal efficiency, specific fuel consumption, specific NO and CO emissions.

2. Geometric Model Development

The specifications of the CAI engine analyzed are given in Table 1. A geometric model of the engine including combustion chamber, intake and exhaust ports, intake and exhaust valves, was structured and meshed for computational domains by using GAMBIT. The computational mesh consisted of 12427 cells at TDC. Figure 1 shows the computational domain of the two-dimensional geometric model at top dead center.

Table 1. Engine Specification

Description	Unit	Value
Bore	[mm]	71.8
Stroke	[mm]	62
Displacement volume	[lt]	0.36
Compression ratio	[-]	10
Intake valve diameter	[mm]	32
Exhaust valve diameter	[mm]	27

3. Model Formulation

The model considered was solved using FLUENT which uses the control-volume-based method to convert the governing equation to algebraic equations. The governing equations of continuity, momentum, energy and the sub-model equations of turbulence, radiation and species transport with finite rate chemistry, auto-ignition and NOx model, which are necessary to simulate the engine cycle were solved in time dependent deforming two-dimensional control volume. The integral form of the conservation equation for ϕ scalar quantity is written for an arbitrary control volume V as follows [17]:

$$\int_V \frac{\partial \rho\phi}{\partial t} dV + \oint \rho\phi\vec{v}.d\vec{A} = \oint \Gamma_\phi \nabla\phi.d\vec{A} + \int_V S_\phi dV \quad (1)$$

where ρ is density, $\vec{v}$ is velocity vector, $\vec{A}$ is surface area vector, Γ_ϕ denotes diffusion coefficient for ϕ and S_ϕ represents source of ϕ per unit volume.

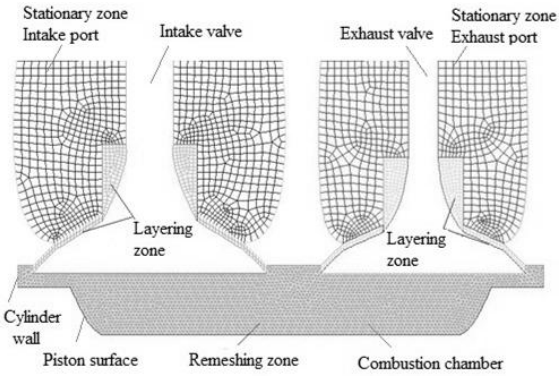

Figure 1. Geometric model structure

3.1. Turbulence model

The RNG k-ε turbulence model was used owing to its degree of accuracy in obtaining the effect of swirling flow. Transport equations for the RNG k-ε are expressed as follows:

$$\frac{\partial}{\partial t}(\rho k)+\frac{\partial}{\partial x_i}(\rho k u_i) = \frac{\partial}{\partial x_j}\left(\alpha_k \mu_{eff}\frac{\partial k}{\partial x_j}\right)+G_k+G_b-\rho\varepsilon-Y_M+S_k \quad (2a)$$

$$\frac{\partial}{\partial t}(\rho \varepsilon)+\frac{\partial}{\partial x_i}(\rho \varepsilon u_i) = \frac{\partial}{\partial x_j}\left(\alpha_\epsilon \mu_{eff}\frac{\partial \varepsilon}{\partial x_j}\right)+C_{1\epsilon}\frac{\varepsilon}{k}(G_k+C_{3\epsilon}G_b)- C_{2\varepsilon}\rho\frac{\epsilon^2}{k}-R_\epsilon+S_\epsilon \quad (2b)$$

In these equations, G_k and G_b denote the generation of turbulence kinetic energy due to mean velocity gradients and buoyancy, respectively. Y_M is the contribution of fluctuating dilatation in compressible turbulence. α_k and α_ε are the inverse effective Prandtl number for k and ε. S_k and S_ε are user-defined source terms. $C_{1\varepsilon}$ and $C_{2\varepsilon}$ are the model constants derived analytically by the RNG theory.

3.2. Species transport and finite-rate chemistry model

Mixing and transport of chemical species can be modeled by conservation equations describing convection, diffusion and reaction

sources for each component species. FLUENT predicts the local mass fraction of each species through the solution of a convection-diffusion equation. The conservation equation for *i* th species is expressed as follows [17]:

$$\frac{\partial}{\partial t}(\rho Y_i)+\nabla.(\rho\vec{v}Y_i)= -\nabla.\vec{j}_i+R_i \qquad (3)$$

where Y_i is the local mass fraction of species *i*, R_i is the net rate of production of species i by chemical reaction and Ji is the mass diffusion of species *i* . Mass diffusion in turbulent flows can be written in the following form:

$$\vec{j}_i=\left(\rho D_{i,m}+\frac{\mu_t}{Sc_t}\right)\nabla Y_i \qquad (4)$$

where, $D_{i,m}$ represents the diffusion coefficient for species i, and Sc_t is the turbulent Schmidt number. The molar rate of creation and destruction of species *i* in reaction *r* for a non-reversible reaction is given by

$$\hat{R}_{i,r}=(v''_{i,r}-v'_{i,r})\left(k_{f,r}\prod_{j=1}^{N}[C_{j,r}]^{(\eta'_{j,r}+\eta''_{j,r})}\right) \qquad (5)$$

where $v''_{i,r}$ and $v'_{i,r}$ are stoichiometric coefficient for product i and reactant i respectively in reaction r. $\eta''_{j,r}$ and $\eta'_{j,r}$ are rate exponent for product j and reactant j respectively in reaction r. $C_{j,r}$ is molar concentration of species j in reaction r, and $k_{f,r}$ is forward rate constant for reaction r. The forward rate constant $k_{f,r}$ is obtained from using the Arrhenius expression given by following,

$$k_{f,r}=A_r T^{\beta} e^{-E/RT} \qquad (6)$$

where

A_r = pre-exponential factor,
β = temperature exponent,
E = activation energy for the reaction,
R = universal gas constant.

Methane combustion involving 6 chemical species in a three step reaction was considered for numerical analysis of the reactions. The required coefficients for the Arrhenius expression are given in Table 2.

The thermal NOx formation was determined by using Zeldovich mechanism and rate constant based on studies of Hanson and Salimian [17].

Table 2.Three step reduced mechanisms of CH_4 combustion [18]

Reaction	A_r	β	E j/kmol	Reaction orders
$CH_4+3/2\,O_2\rightarrow CO+2H_2O$	5.010^{11}	0	2.010^{8}	$[CH_4]^{0.7}[O_2]^{0.8}$
$CO+1/2\,O_2\rightarrow CO_2$	2.210^{6}	0	4.210^{7}	$[CO][O_2]^{0.25}[H_2O]^{0.5}$
$CO_2\rightarrow CO+1/2\,O_2$	1.110^{13}	-0.97	3.310^{8}	$[CO_2][H_2O]^{0.5}[O_2]^{-0.25}$

3.3. Initial and Boundary Condition

The numerical simulation was started at intake valve closing time (IVC) after one cycle for distributions of the species forming a mixture in cylinder. The temperature was considered as 570 K at IVC in order to reach an auto ignition thermal condition for all cases. The temperatures of the cylinder wall, cylinder head and piston head were also set to 420 K, 440 K and 460 K respectively. Pressures in cylinder at IVC were obtained from first cycle of the simulation with atmospheric pressure boundary condition.

The thermodynamic properties of mixing gas in the cylinder were considered as a constant value for viscosity and thermal conductivity, the ideal gas law for density and specific heat values at constant pressure(c_p) also depending upon both the temperature and concentration of species. EGR rates in the mixture were calculated considering the methane combustion mechanism. Since EGR includes product species, CO_2, H_2O, N_2 and O2, the EGR rate was calculated by,

$$y\, m_{EGR}=\frac{m_{EGR}}{m_{react}+m_{EGR}} \qquad (7)$$

where m_{react} is the amount of methane and air by mass, m_{EGR} is the amount of EGR.

The simulations were run at 1500 rpm engine speed that is one of the most common driving ranges. The computational time step used is 0.1 CAD corresponding to $1.11x10^{-5}$ sec, which is enough to time step independent solution [19]. It was also considered as converge criteria, 10^{-7} for energy and 10^{-4} for other scalars.

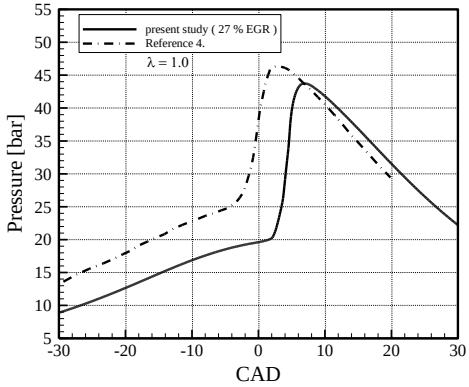

Figure 2. Comparison of in-cylinder pressure traces

4. Model Validation

Pressure is fundamental parameter that can be measured directly inside a cylinder of an engine. Therefore, in-cylinder pressure values obtained from this numerical study may be validated by comparing with some experimental studies. For this purpose, we considered the investigation of Cho et al.[4],studied on rapid intake compression and exhaust machine at compression ratio of 11.7 to determine the effect of internal EGR rate on CAI in methane engine combustion.
Fig. 2 illustrates comparison of in-cylinder pressure traces. Pressure trace for Reference 4. It is for an EGR rate of %30 and equivalence ratio value of 1. It can be seen that when the peak pressure value in the current model is compared to that of Reference 4, it is reasonable to estimate data for intended purposes of this study.

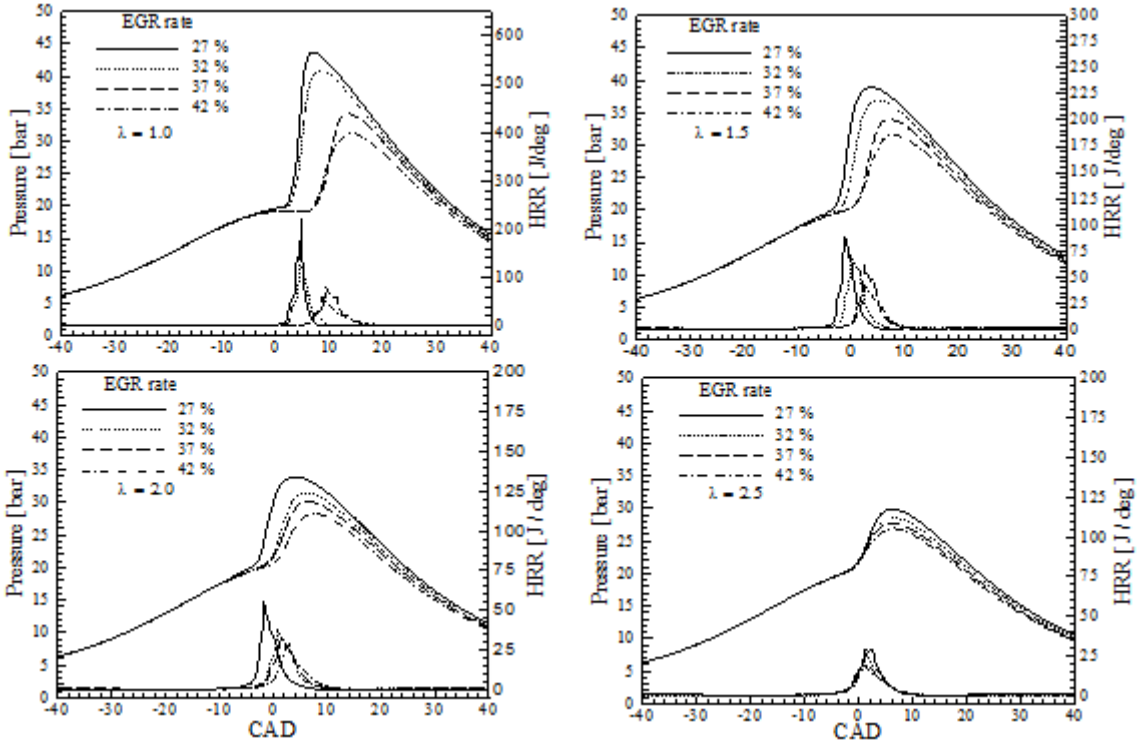

Figure 3. In-cylinder pressure and heat release rate versus the CAD for different EGR rates and λ values

5. Results and Discussion

5.1. In-cylinder pressure and heat release rate

Figure 3 shows the in-cylinder pressure and heat release rate values versus the CAD with different EGR rates and excess air ratios (λ) at 1500 rpm. As seen in these figures, the values of the highest peak pressure for each excess air ratio were obtained at an EGR rate of 27 %. These values are 43.72 bar at 7 CAD, 38.96 bar at 3.8 CAD, 33.91 bar at 4 CAD and 29.88 bar 6.1 CAD after top dead center position (ATDC) respectively. The lowest peak pressure is 27.21bar at 5.6 CAD ATDC at an EGR rate of 42% with excess air

ratio of 2.5.

Heat release rate (HRR) is a measure of how fast the chemical energy of the fuel is converted to thermal energy. Therefore, it directly affects the pressure rise rate (dP/dt). The heat release rate was calculated using the first law of thermodynamics as given in [21], as follows:

$$\frac{dQ_{hr}}{d\theta} = \frac{\gamma}{\gamma\text{-}1} P \frac{dV}{d\theta} + \frac{1}{\gamma\text{-}1} V \frac{dP}{d\theta} + \frac{dQ_w}{d\theta} \qquad (8)$$

where, γ, θ, Q_W, P and V are specific heat ratio (c_p/c_v), the crank angle, heat loss from the cylinder walls, cylinder pressure and cylinder volume respectively.

When the heat release rate curves given in Figure 3 are compared, the heat release rate (HRR) at an EGR rate of 27 % for each excess air ratio is the highest value.

As expected, HRR has a tendency to decrease with increase of EGR rate and excess air ratio. Heat release rate increased abruptly and reached the value of 220.15 J/deg at 4.6 CAD-BTDC (before top dead center) at EGR rate of 27% with λ=1. This brought about high pressure rise rate, which leads to knocking combustion. Pressure rise rate (PRR) is a significant parameter to indicate knock intensity throughout the engine cycle. The threshold value of the PRR $(dP/dt)_{max}$ causing of knocking combustion in this study was considered as 5 MPa/ms corresponding to 5.5 bar/CA for an engine operating at 1500 rpm[20].

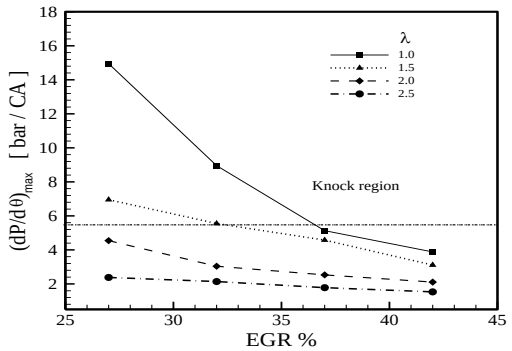

Figure 4. Pressure rise rate $(dP/d\theta)_{max}$ versus the EGR rate

Figure 4 illustrates the maximum pressure rise rate $(dP/d\theta)_{max}$ values versus the EGR rate for different λ values. The maximum pressure rise rate at an EGR rate of 27 % and 32 % for λ=1 and λ =1.5, exceeds the limit value of PRR leading to knocking combustion, despite the fact that there are no pressure fluctuations in pressure traces. It is also noticed that the dominant effect of EGR rate on reduction of pressure rise rate decreases when the λ value increases.

5.2. In-Cylinder Temperature

In-cylinder temperature traces are displayed in Fig. 5.The highest in-cylinder temperature is 2645.43 K at 7.6 CAD- ATDC at an EGR rate of 27 % with λ =1. The reason for such a high value temperature is the instantaneous heat release rate increase in the mixture, being stoichiometric (λ=1) and including a lower EGR rate.

EGR rate has heat capacity and dilution effects on temperature decrease, which absorbs heat due to higher heat capacity value and reduces the concentration of the fuel in the mixture. Fig. 5 shows that CAI combustion temperature can be kept at a low value by means of the increasing EGR rate and a leaner mixture. Thus, the lowest in-cylinder temperature was obtained at an EGR rate of 42 % with λ=2.5.

5.3. Combustion Duration

Since in the CAI combustion process, ignition timing cannot be controlled directly like SI and CI, it is necessary to supply the required condition for auto-ignition in the cylinder. In addition, auto-ignition must be initiated at the right time to attain optimum engine performance and to control the combustion process.

Fig. 6 shows combustion duration calculated by crank angle interval between the points at which 5 % to 95 % of the fuel was consumed [6],[21].As seen in Figure 6, the combustion duration varied from 5 to 23 CAD, dependent on EGR rate and excess air ratio. Combustion duration was prolonged by increasing both EGR and excess air ratio due to lower temperature in cylinder.

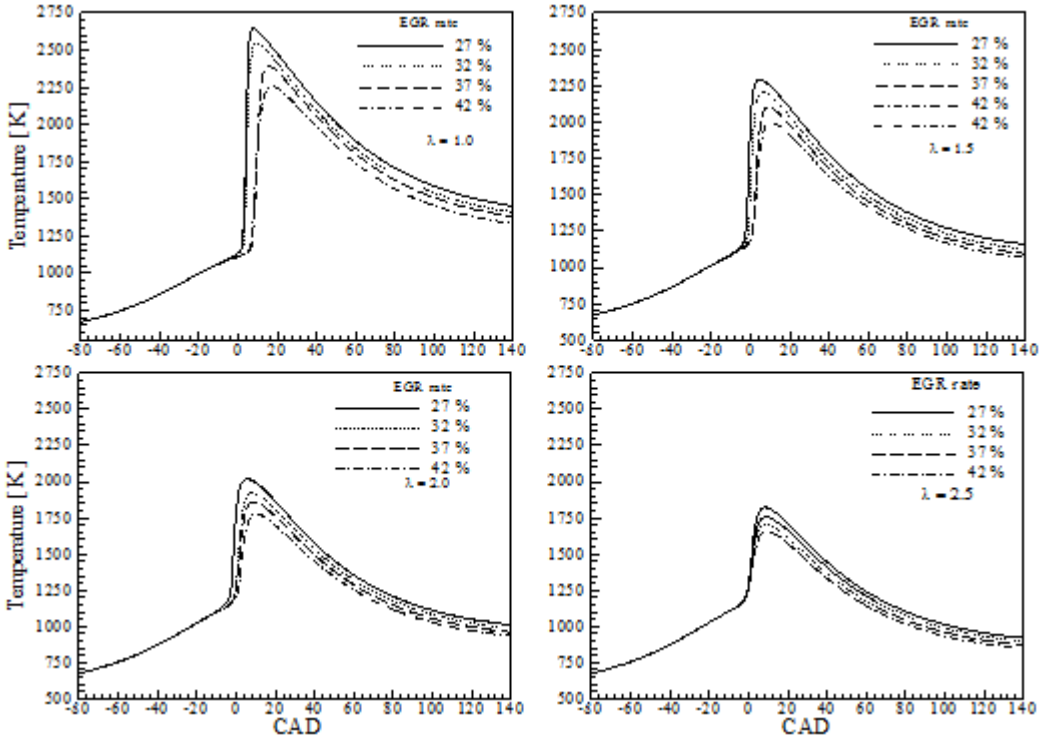

Figure 5. In-cylinder pressure and heat release rate versus the CAD for different EGR rates and λ values

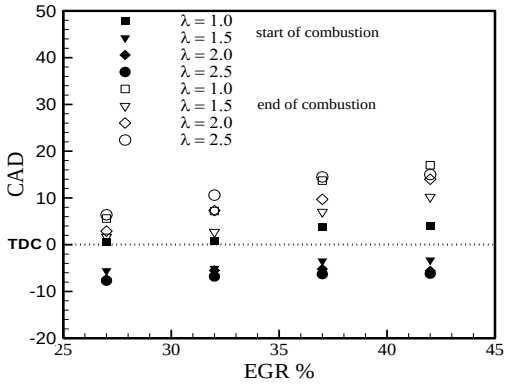

Figure 6. Combustion duration versus the EGR rate

5.4. Thermal efficiency and specific fuel consumption

Thermal efficiency is defined as the ratio of the brake work W_b by input fuel energy. W_b was calculated by the following equation[21]:

$$W_b = \eta_m . W_i \quad (9)$$

where, η_m is mechanical efficiency and W_i is indicated work, calculated by equation,

$$W_i = \int P . dV \quad (10)$$

In this equation, P is pressure and dV is volume displacement. Input fuel energy is also calculated from equation 14.

$$Q_{in} = m_f . H_{LV} \quad (11)$$

where, m_f is fuel mass and H_{LV} is the lower heating value of fuel. Thermal efficiency is, thus, calculated as follows:

$$\eta_{th} = \frac{W_b}{Q_{in}} \quad (12)$$

The results of break work, thermal efficiency, and specific fuel consumption values are given in Tables 3. Based on these results, with the increase of EGR rate for λ value of 2 and 2.5, the thermal efficiency values are in declining trend. For λ values of 1 and 1.5, the thermal efficiency rises and then it tends to decrease. On the other hand, the rise of EGR rate caused a increase of specific fuel consumption for λ values of 2.0 and 2.5. With the increase of excess air ratio, thermal efficiency increased. Afterwards it had a decreasing trend, while specific fuel consumption decreased and then increased.

5.5. Emissions

NOx emission consists of mostly nitric oxide (NO). NOx formation is very sensitive to in–cylinder temperature history. At temperature over 2200 K, NOx formation increases significantly [17],[22]. Fig.7 shows the specific NOx emission obtained in this study. The highest specific NOx emission was

obtained as $5.45x10^{-3}$ mg /J at an EGR rate of 27 % with λ=1. The lowest SNOx emission value, $1.98x10^{-7}$ mg /J, was obtained at an EGR rate of 42 % with λ value of 2.5. It is also noticed that the effect of EGR on reducing NOx emission decreased with increase of excess air ratio value.

Table 3.Results for various EGR rates and λ values

EGR Rate [%]	W_b [J]	SFC [mg /J]	η_{th}	W_b [J]	SFC [mg /J]	η_{th}
	λ=1.0			λ=1.5		
27	143.43	0.0589	0.314	100.40	0.0570	0.324
32	136.26	0.0582	0.318	94.52	0.0568	0.325
37	125.82	0.0589	0.314	88.71	0.0565	0.327
42	116.66	0.0591	0.312	82.54	0.0567	0.326
	λ=2.0			λ=2.5		
27	76.01	0.0564	0.328	61.00	0.0565	0.327
32	71.09	0.0567	0.326	56.15	0.0578	0.320
37	66.50	0.0569	0.325	51.27	0.0591	0.313
42	60.32	0.0584	0.317	47.35	0.0597	0.309

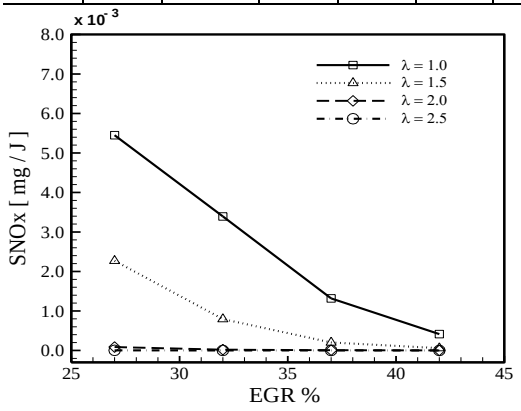

Figure 7. Specific NOx emission values versus %EGR

The results of specific CO emission values are also illustrated in Figure 8. The SCO emission values increased when the EGR rate increased for λ values of 1.5, 2.0 and 2.5. However, at λ=1, the zone remaining at a low temperature because of shorter combustion duration had a dominate effect on increase of CO emission. Thus, SCO emission at an EGR rate of 27 % for λ=1 reached a value of $0.82x10^{-5}$ mg/J. The maximum SCO emission value, $2.55x10^{-4}$ mg /J, was obtained at EGR rate of 42 % with an λ value of 2.5 due to lower temperature leading to reduced oxidation from CO to CO_2.

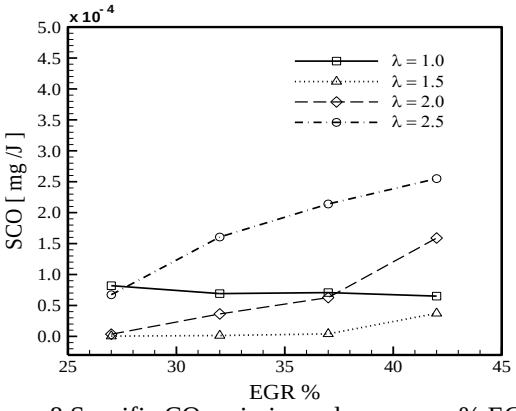

Figure 8.Specific CO emission values versus % EGR

6. Conclusions

The effect of exhaust gas recirculation (EGR) on controlled auto-ignition (CAI) considering the same temperature at intake valve closing time for all cases was evaluated by using the CFD code FLUENT program. Various EGR rates and excess air ratios were applied to investigate their effects on controlled auto-ignition in a methane fueled engine. The following conclusions were obtained from this study.

The pressure value increases with the decrease in EGR rate, which leads to an increase in the knock intensity based on pressure rise rate because the instantaneous heat release rate increases. The pressure rise rate at an EGR rate of 27 % and 32 % for λ values of 1.0 and 1.5 is more than 5.5 MPa/CA. These operation conditions were, therefore, considered in the knock combustion region.

The rise of the EGR rate reduced the temperature in the cylinder due to its heat capacity and dilution effect, because EGR includes species, CO_2 and H_2O which have higher heat capacity and cause the fuel concentration to be lower. When the excess air ratio increased, the temperature decreased because of the dilution effect. CAI combustion resulted in a higher temperature in the case of the stoichiometric and lean (for λ=1.5) mixture with a lower EGR rate (up to 37 %).

The combustion duration increased with the rise of EGR rate and excess air ratio, because

the temperature decreased in the cylinder, which leads to slower combustion velocity. The start time of combustion retarded, since the end of compression temperature decreased due to the reduction of ratio of specific heats with increase of EGR rate. In contrast, with the increase in excess air ratio, the start time of combustion time advanced.

The thermal efficiency for λ values of 2 and 2.5 had a declining trend when EGR rate increased. At λ values of 1 and 1.5, with rise of EGR rate, the thermal efficiency increased and then decreased. The highest thermal efficiency was found at an λ value of 2 with an EGR rate of 27 %.

Although CAI combustion has lower NOx emission potential, NOx formation can have a higher level when the rapid heat release rate results in a very high temperature value in the cylinder. The results show that at an EGR rate up to 32 % for λ values of 1 and 1.5, the SNOx emission value is very high and has an unacceptable level because of high temperature. However, it decreased considerably after an EGR rate of 32 % for λ values of 1 and 1.5. Lower SNOx values at EGR rate up to 32 % were also achieved by further increasing the λ value. The lowest SNOx emission was found at an EGR rate of 42 % for λ =2.5 with higher SCO emission penalty.

Acknowledgment

The authors would like to thank the Scientific and Technological Research Council of Turkey for its financial support (TUBITAK, Project Number 113M101).

7. References

[1] T.Chen, H. Xie, L.Li, L.Zhang, X.Wang, H.Zhao,"Methods to achieve HCCI/CAI combustion at idle operation in a 4VVAS gasoline engine," Applied Energy., 2014 (116):41-51

[2] Zhao H. Motivation definition and history of HCCI/CAI engines. In: Zhao H, editor. HCCI and CAI Engines for the Automotive Industry. Woodhead Publishing Limited; 2007.

[3] N. Kalian, H. Zhao, J. Qiao, "Investigation of transition between spark ignition and controlled auto-ignition combustion in a V6 direct-injection engine with cam profile switching," Automobile Engineering Journal., 2008(222):1911-26.

[4] G.Cho, G.Moon, D.Jeong, C. Bae, "Effects of internal exhaust gas recirculation on controlled auto-ignition in methane engine combustion," Fuel., 2009(88):1042-48.

[5] C.H. Lee, K.H. Lee, "An experimental study of the combustion characteristics in SCCI and CAI based on direct-injection gasoline engine," Experimental Thermal and Fluid Science, 2006(31):1121-32.

[6] J.Hunicz, P. Kordos, "An experimental study of fuel injection strategies in CAI gasoline engines," Experimental Thermal and Fluid Science., 2010 (35):243-52.

[7] Y.Bai, Z. Wang,J. Wang, "Part–load characteristics of direct injection spark ignition engine using exhaust gas trap," Applied Energy., 2010(87):2640-46.

[8] P.G. Aleiferis, M.F. Rosati, "Controlled auto ignition of hydrogen in a direct injection optical engine," Combustion and Flame.,2012(159): 2500-15.

[9] L.Shi, K. Deng, Y. Cui, S. Qu, W. Hu, "Study on knocking combustion in a diesel HCCI engine with fuel injection in negative valve overlap," Fuel., 106(2013): 478-483.

[10] L. Cao, H. Zhao, X. Jiang, "Analysis of controlled auto-ignition/HCCI combustion in direct injection engine with single and split fuel injections," Combustion Science and Technology., 2007(180)176-205.

[11] Zhao H. Overview of CAI/HCCI gasoline engines. In: Zhao H, editor. HCCI and CAI Engines for the Automotive Industry. Woodhead Publishing Limited; 2007.

[12] D.Yap,J. Karlovsky, A. Megaritis, M.L. Wyszynski, H. Xu, "An investigation into propane homogeneous charge compression (HCCI) engine operation with residual gas trapping," Fuel, 84(2005): 2372-79.

[13] J. Li, H. Zhao, N. Ladommatos, "Performance and analysis of a four-stroke multicylinder gasoline engine with CAI combustion," SAE Paper. 2001-01- 3608.
[14] M.Fathi, R.K. Saray, M.D. Checkel, "The influence of exhaust gas recirculation (EGR) on combustion and emissions of n-heptane/natural gas fueled homogeneous charge compression ignition (HCCI) engines," Applied Energy., 2011(88)4719-24.
[15] M. Ghorbanpour, R.A. Rasekhi, "A parametric investigation of HCCI combustion to reduce emissions and improve efficiency using a CFD model approach," Fuel., 106(2013): 157-165.
[16] R.Chen, N.Milovanovic, "A computational study into the effect of exhaust gas recycling on homogeneous charge compression ignition combustion in internal combustion engine fuelled with methane," International Journal of Thermal Sciences.,2002(41) 805-13.
[17] Fluent 6.3 User's Guide, 2006. Fluent Incorporated, Centerra Resource Park, 10. Cavendish Court,Lebanon, NH 03766,USA.
[18] Johansen, L. C. R. Rans Simulation of Oxy-Natural Gas Combustion. Aalborg University, M.S. Thesis, Denmark, 2010.
[19] G.M.Kosmadakis,C.D.Rakopoulos, . Demuynck, M.D.Paepe, S.Verhelst, " CFD modeling and experimental study of combustion and nitric oxide emissions in hydrogen-fueled spark ignition engine in very wide range of EGR rates" Hydrogen Energy., 37 (2012):10917-34.
[20] R.K. Maurya, A.K. Agarwal, "Experimental investigation on effect of intake air temperature and air-fuel ratio on cycle-to-cycle variations of HCCI combustion and performance," Applied Energy, 2011(88)1153-63.
[21] Stone R. Introduction to Internal Combustion Engines, Third Edition. Society of Automotive Engineers Inc., Warrendale, 641 pp, 1999.
[22] M. Yao, Z. Zheng, H. Liu, "Progress and recent trend in homogeneous charge compression ignition (HCCI) engines," Progress in Energy and Combustion Science., 2009; 35: 398-437.